Observation of the Crossover from Photon Ordering to Delocalization in Tunably Coupled Resonators

Michele C. Collodo,[1,*] Anton Potočnik,[1] Simone Gasparinetti,[1] Jean-Claude Besse,[1] Marek Pechal,[1] Mahdi Sameti,[2] Michael J. Hartmann,[2] Andreas Wallraff,[1] and Christopher Eichler[1]

[1]*Department of Physics, ETH Zurich, CH-8093 Zurich, Switzerland*
[2]*Institute of Photonics and Quantum Sciences, Heriot-Watt University Edinburgh EH14 4AS, United Kingdom*

Networks of nonlinear resonators offer intriguing perspectives as quantum simulators for nonequilibrium many-body phases of driven-dissipative systems. Here, we employ photon correlation measurements to study the radiation fields emitted from a system of two superconducting resonators in a driven-dissipative regime, coupled nonlinearly by a superconducting quantum interference device, with cross-Kerr interactions dominating over on-site Kerr interactions. We apply a parametrically modulated magnetic flux to control the linear photon hopping rate between the two resonators and its ratio with the cross-Kerr rate. When increasing the hopping rate, we observe a crossover from an ordered to a delocalized state of photons. The presented coupling scheme is intrinsically robust to frequency disorder and may therefore prove useful for realizing larger-scale resonator arrays.

Engineering optical nonlinearities that are appreciable on the single photon level and lead to nonclassical light fields has been a central objective for the study of light-matter interaction in quantum optics [1–3]. While such nonlinearities have first been realized in individual optical cavities [4,5] and with Rydberg atoms [6,7], more recently superconducting circuit quantum electrodynamics (QED) [8] has proven to be a powerful platform for the study of nonclassical light fields. Circuit QED systems facilitate strong effective interactions between individual photons [9,10], long coherence times [11], as well as precise control of drive fields [12,13] within a large variety of possible design implementations. Particularly, *in situ* tunable or nonlinear couplers have been explored more recently for superconducting elements [14–21].

Well-controllable engineered quantum systems offer interesting perspectives to study interacting many-body systems with photons [22–24]. Interacting photons are typically explored in a nonequilibrium regime, in which continuous driving compensates for excitation loss and yields stationary states of light fields [25].

Nonequilibrium coupled resonator systems have been investigated experimentally, both in a semiclassical and in a quantum regime. Macroscopic self-trapping of exciton polaritons has been observed in a dimer of coupled Bragg stack microcavities [26], vacuum squeezing was demonstrated in a dimer of superconducting resonators [27], the unconventional photon blockade has been observed in the microwave and the optical domain [28,29], and signatures of bistability have been found in a chain of superconducting resonators [30]. Moreover, a transition from a classical to a quantum regime has been

observed in the decay dynamics of a resonator dimer [31], chiral currents of one or two photons have been generated in a three qubit ring [32], and spectral signatures of many-body localization [33] as well as a Mott insulator of photons [34] have been observed in a qubit chain.

In this Letter, we explore the interaction between individual photons in a driven-dissipative system of two nonlinearly coupled superconducting resonators [see Fig. 1(a)]. The nonlinear coupler mediates a cross-Kerr interaction V, on-site Kerr interactions U_a and U_b, and an effective linear hopping interaction with *in situ* tunable rate J_{ac}. Our experiment provides a realization of a steady state quantum system, in which cross-Kerr interactions exceed local Kerr interactions, meaning that the force between particles grows as they are separated and only starts to decay once the separation exceeds the lattice constant. We measure the on-site $g_{aa}^{(2)} := g_{aa}^{(2)}(\tau = 0)$ and cross correlations at zero time delay $g_{ab}^{(2)} := g_{ab}^{(2)}(\tau = 0)$ between the emitted field from both resonators. In the limit of small J_{ac}/V, a photon trapped in one resonator blocks the excitation of the neighboring resonator and vice versa, leading to a spontaneous self-ordering of microwave photons [35,36]. Such an intersite photon blockade regime has been predicted for resonator arrays with nonlinear couplers [37,38]. When increasing J_{ac}/V, however, a delocalization of photons and a simultaneous occupation of both resonators becomes favorable, leading to a change in the photon statistics.

For this experiment we utilize an on-chip superconducting circuit consisting of two lumped element resonators with characteristic impedance $Z = 80 \ \Omega$ [see Figs. 1(b),1(c)]. The aforementioned nonlinear coupling circuit, interconnecting
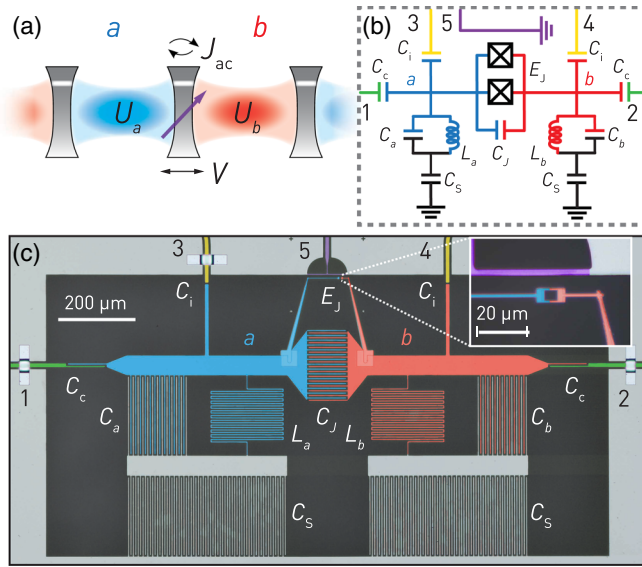
FIG. 1. (a) Sketch of an optical analogue of the setup, consisting of two resonator modes a and b with Kerr nonlinearities U_a and U_b, coupled via a cross-Kerr interaction V and a tunable linear hopping rate J_{ac}. (b) Equivalent circuit diagram and (c) false-colored micrograph of the sample, featuring two lumped-element LC resonators a, b (blue, red), coupled via a nonlinear coupling element composed of a capacitor and a SQUID (inset). The resonators are accessed via two symmetric sets of weakly coupled input lines (yellow, ports 3 and 4) and output lines (green, ports 1 and 2). A flux modulation tone is applied via a dedicated T-shaped flux line (purple, port 5).
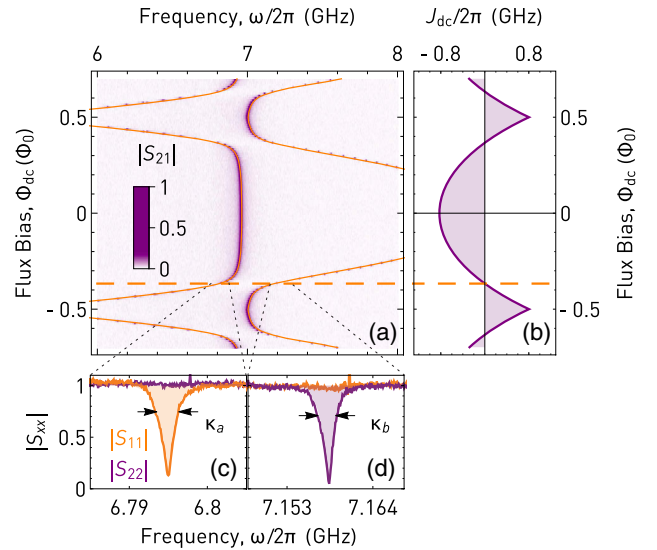

FIG. 2. (a) Measured transmission amplitude $|S_{21}|$ vs magnetic flux Φ_{dc} and fit of the resonance frequencies to a linear circuit impedance model (thin orange line). The working point $J_{dc} = 0$ is indicated by a dashed orange line. (b) Linear hopping rate J_{dc} vs Φ_{dc}, calculated using a normal mode model based on the circuit parameters extracted from (a). (c),(d) Reflection coefficient measurements of bare cavity modes at $\Phi_{dc} \approx -0.37\Phi_0$ ($J_{dc} \approx 0$) with fit to a Lorentzian (solid filling).

the two resonators, consists of a capacitively shunted superconducting quantum interference device (SQUID) with capacitance $C_J = 95$ fF and Josephson energy $E_J^{max}/h = 80$ GHz, with the Planck constant h. We use a superconducting coil and an on-chip flux drive line (port 5) to ensure full dc and ac control of the magnetic flux threading the SQUID loop. Each resonator is weakly coupled to an input port (3 and 4), through which we drive the system, and to an output port (1 and 2) into which approximately 50% of the intracavity field is emitted and measured using a linear detection chain. The total decay rates are measured to be $(\kappa_a, \kappa_b)/2\pi = (2.8, 2.4)$ MHz.

First, we characterize the sample by measuring the transmitted amplitude $|S_{21}|$ as a function of external magnetic flux Φ_{dc}. At each flux bias point we observe two resonances corresponding to the two eigenmodes of the system, see Fig. 2(a). The flux dependence of the measured eigenfrequencies is well explained by a linear circuit impedance model comprising a tunable effective Josephson energy, which allows us to determine the aforementioned circuit parameters. From a normal mode model we extract the tuning range of the corresponding linear hopping rate $J_{dc}/2\pi = -0.8...0.8$ GHz [Fig. 2(b)]. The tunability of J_{dc} results from an interplay between the capacitive and the flux-dependent inductive coupling between the two resonators. As these carry opposite signs, we are able to cancel both contributions

achieving approximately zero net static linear coupling $J_{dc} \approx 0$ at a dc flux bias point of $\Phi_{dc} \approx -0.37\,\Phi_0$, where $\Phi_0 = h/2e$ is the magnetic flux quantum. At this bias point the two measured resonances $(\omega_a, \omega_b)/2\pi = (6.802, 7.164)$ GHz are separated by the bare detuning $\Delta/2\pi \equiv (\omega_b - \omega_a)/2\pi = 362$ MHz and correspond closely to the local modes of the system [Figs. 2(c),2(d)]. As a result, the radiation of each mode (a, b) is collected in its respective output line at port (1, 2). Notably, the finite detuning Δ between the bare cavity modes suppresses undesired nonlinear interactions, which would otherwise give rise to pair hopping and correlated hopping and disrupt the scope of the experiment (see Supplemental Material [39]).

In order to recover a well-controllable linear hopping rate despite the finite cavity detuning, we implement a parametric coupling scheme [14,19,43]. Here, we apply an ac modulated flux drive to the SQUID with a variable amplitude Φ_{ac} and a modulation frequency ω_{ac}, which equals the resonator detuning $\omega_{ac} = \Delta$. For $\Phi_{ac} = 0$ we recover the uncoupled resonator modes when probing the transmission spectra $|S_{13}|$ and $|S_{24}|$ [see Fig. 3(a)]. However, as we increase Φ_{ac}, we observe a simultaneous frequency splitting of both modes, which scales linearly with Φ_{ac}, and which we interpret as the result of a parametrically induced photon hopping with rate $J_{ac}/2\pi = 0...40$ MHz (see Supplemental Material [39]).

In an appropriate doubly rotating frame, where each mode rotates at its resonance frequency, our system is well described by an effective Hamiltonian
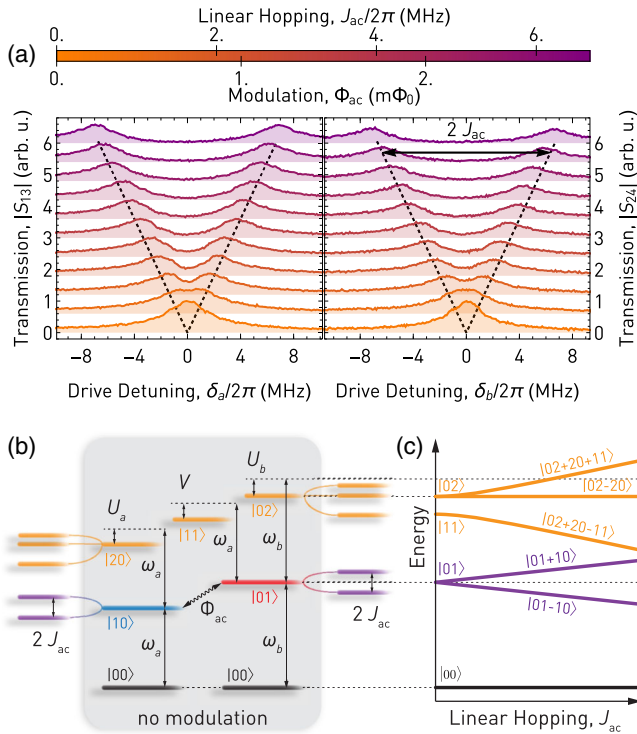
FIG. 3. (a) Measured transmission amplitude $|S_{13}|$ ($|S_{24}|$) through resonator a (b) for varying flux modulation amplitude Φ_{ac} applied to port 5. Linear fits to the resonance frequencies of the J_{ac}-hybridized modes are shown as black dashed lines. (b) Energy level diagram for vanishing (gray box) and finite linear hopping rate J_{ac} via parametric modulation at the frequency difference $\Delta = \omega_b - \omega_a$. (c) Energy levels of resonator b in the first (purple) and second (orange) excitation manifold vs J_{ac}.
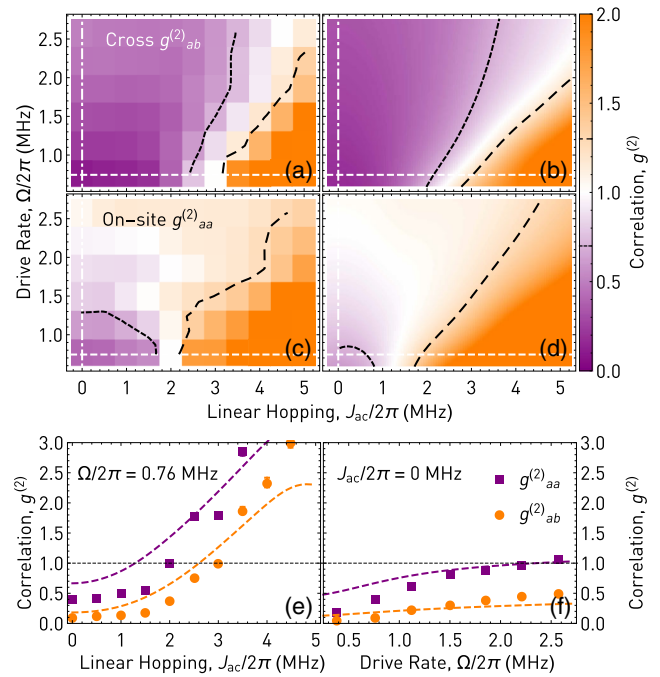
FIG. 4. (a),(c) Measured cross (on-site) second order photon correlator $g_{ab}^{(2)}$ ($g_{aa}^{(2)}$) as a function of the linear hopping rate J_{ac} and the drive rate Ω; the black dotted (dashed) line indicates the linearly interpolated contour for $g^{(2)} = 0.7$ ($g^{(2)} = 1.3$). (b),(d) Corresponding results from numerical simulations. (e) $g^{(2)}$ vs J_{ac}, cut for $\Omega/2\pi = 0.76$ MHz (see white dashed line; measured data are shown with markers, numerical simulations with dashed lines). (f) $g^{(2)}$ vs Ω, cut for $J_{ac}/2\pi = 0$ MHz (see white dash-dotted line).

$$\frac{1}{\hbar}\mathcal{H}_\Delta = \delta_a a^\dagger a + \delta_b b^\dagger b + J_{ac}(a^\dagger b + b^\dagger a)$$
$$+ \frac{1}{2}U_a a^{\dagger 2} a^2 + \frac{1}{2}U_b b^{\dagger 2} b^2 + V a^\dagger a b^\dagger b$$
$$+ \Omega_a(a^\dagger + a) + \Omega_b(b^\dagger + b),$$

with the drive detuning $\delta_i = \omega_{\text{drive},i} - \omega_i$ ($i \in \{a, b\}$) and the drive rates Ω_i. The on-site and the cross-Kerr interaction rates at zero coupling bias are $(U_a, U_b, V)/2\pi = -(3.1 \pm 0.3, 2.7 \pm 0.2, 7.0 \pm 0.3)$ MHz, which have been extracted from a spectroscopic measurement (see Supplemental Material [39]). In the absence of a parametric modulation the eigenstates of this Hamiltonian correspond to the photon number states $|n_a n_b\rangle$ in the local basis [compare Fig. 3(b)]. The second order transitions are redshifted by the corresponding Kerr rates. For finite J_{ac} the eigenstates hybridize in both the one- and two-photon manifold.

We focus on a parameter regime in which $|V|$ and J_{ac}, as well as κ_i and Ω_i, are comparable in magnitude, featuring a competition between nonlinear interaction and linear hopping, as well as between drive and dissipation. In our system we additionally have $|U_i| \approx \kappa_i$. Both $\Omega_a = \Omega_b = \Omega$,

setting the average number of excitations in the system, and J_{ac}, setting the rate at which the resonators exchange excitations, are utilized as tunable control parameters, while V, U_i, and κ_i are constant. In the experiment we keep the drive frequencies, and thus $\delta_i = 0$, fixed. We eliminate influences of the phase of J_{ac} on the measured results by averaging over multiple randomized phase configurations.

We characterize the quantum states of the uniformly and continuously driven two-resonator system by measuring the second order cross $g_{ab}^{(2)}$ and on-site correlation $g_{aa}^{(2)}$ of the emitted radiation as a function of J_{ac} and Ω [see Figs. 4(a),4(c)]. To this aim, we linearly amplify and digitize the radiation fields at both output ports in order to obtain the second order photon correlations [27,44,45]. To enhance the signal-to-noise ratio, we use a quantum-limited Josephson parametric amplifier [27] operated in a phase-sensitive mode (see Supplemental Material [39] for details about the detection process). The measured $g^{(2)}$ correlations are compared with the results of a numerical master equation simulation [46] [see Figs. 4(b),4(d)]. As confirmed by this simulation, the average resonator occupations remain at or below the single photon level for all the data presented in Fig. 4.

In the regime of small J_{ac} and low Ω we measure the radiation to be antibunched, see Fig. 4. In this limit, the cross-Kerr interaction effectively shifts the transition frequency of one cavity when a photon is present in the other and thus detunes the ($|01\rangle, |10\rangle \leftrightsquigarrow |11\rangle$) transition from the drive tones. This inhibits simultaneous occupation of both cavities, leading to a dynamic self-ordered photon state manifested as antibunching in the photon cross statistics. We thus observe the finite lattice size version of the spontaneous breaking of the symmetry between the two cases of only even or only odd lattice sites being occupied [37,47]. Equivalently, the on-site Kerr interaction prevents each mode from being doubly excited, leading to antibunched on-site correlations.

Increasing the hopping rate J_{ac} results in a hybridization of the modes in both the one- and two-excitation manifold; see Fig. 3(c) for a level diagram as a function of J_{ac}. When J_{ac} becomes comparable to the Kerr rate $|U_i|$, the transitions to the single photon manifold become detuned from the drive frequency, while the two-photon transition to the symmetric $|02 + 20 + 11\rangle$ branch becomes resonant with the drive. This leads to a more efficient drive into the second excitation manifold compared to the originally dominant single photon states and to an admixture of simultaneous cavity occupations ($|11\rangle$, $|20\rangle$, and $|02\rangle$). This causes a crossover from antibunched to bunched statistics in both the measured $g_{ab}^{(2)}$ and $g_{aa}^{(2)}$, see Fig. 4(e). Interestingly, we find a regime in which the on-site correlation $g_{aa}^{(2)}$ is already close to unity, while the cross-correlation $g_{ab}^{(2)}$ is still antibunched. We attribute this effect to $|V|$ being larger than $|U_i|$. Whereas the observed anticorrelated $g^{(2)}$ functions are expected to persist for larger lattices, the bunching at large linear coupling is a finite size effect as no spectrally dense single excitation band forms for two resonators.

Studying the dependence on the drive rate Ω, we find that $g_{aa}^{(2)}$ approaches unity when Ω exceeds $|U_i|$ [Fig. 4(f)], which we explain by the breakdown of the photon blockade. This effect is found to be largely independent of J_{ac}. We observe a similar behavior for the cross-correlations. In this case, however, the measured $g_{ab}^{(2)}$ approaches one-half in the limit of large drive rate Ω, which is in good agreement with the result obtained from the numerical simulations.

In conclusion, we have realized a coupled cavity system, featuring a tunable ratio between linear hopping and cross-Kerr interaction rate and observed the crossover from photon ordering to delocalization. Inspired by the proposals by Jin et al. [37,38], we interpret the measured cross correlations as an order parameter in a (J_{ac}, Ω)-dependent phase diagram of the system. The observed crossover closely resembles the onset of a driven-dissipative photon ordering phase transition, from a fully ordered crystalline phase dominated by spontaneous symmetry breaking towards a uniform delocalized steady-state phase [48,49].

As such, we demonstrated the feasibility to measure and control nonequilibrium quantum many-body phenomena using interacting photons in engineered quantum systems [50]. Such strongly correlated photonic systems may prove particularly useful as a tool for analog quantum simulation [51–54], where the active control of extended quantum gases may be used to emulate other less accessible quantum systems, with the prospect of complementing theoretical and numerical studies in gaining insights on exotic quantum phenomena [55–59].

We expect the demonstrated coupling mechanism to be well extendable towards larger resonator arrays. Resilience to disorder in electrical parameters [60] and suppression of potential crosstalk can be achieved by frequency staggering of neighboring cavities along with the adjustability of the parametric modulation frequencies. Additionally, the employed lumped element structures excel in this scenario thanks to a compact footprint and high design versatility.

The presented system and variations thereof could be used to explore regimes in which intersite interactions exceed on-site interactions [61,62]. Additionally, the controllability of the phase of the hopping rate could be employed to create artificial gauge fields in plaquette systems and to study nonreciprocal dynamics with photons [32]. Furthermore, the variability of flux modulation frequencies could enable the controllable activation of additional interaction terms such as a parametric coupling between neighboring resonators [63] or pair hopping [64], e.g., for the study of supersolid phases [65,66].

---

* michele.collodo@phys.ethz.ch

[1] S. Haroche and J. M. Raimond, *Exploring the Quantum: Atoms, Cavities, and Photons* (Oxford Graduate Texts, Oxford University Press, Oxford, 2013).

[2] J. M. Raimond, M. Brune, and S. Haroche, Manipulating quantum entanglement with atoms and photons in a cavity, Rev. Mod. Phys. **73**, 565 (2001).

[3] D. E. Chang, V. Vuletić, and M. D. Lukin, Quantum nonlinear optics—photon by photon, Nat. Photonics **8**, 685 (2014).

[4] R. J. Thompson, G. Rempe, and H. J. Kimble, Observation of Normal-Mode Splitting for an Atom in an Optical Cavity, Phys. Rev. Lett. **68**, 1132 (1992).

[5] K. M. Birnbaum, A. Boca, R. Miller, A. D. Boozer, T. E. Northup, and H. J. Kimble, Photon blockade in an optical cavity with one trapped atom, Nature (London) **436**, 87 (2005).

[6] M. Brune, F. Schmidt-Kaler, A. Maali, J. Dreyer, E. Hagley, J. M. Raimond, and S. Haroche, Quantum Rabi Oscillation:

A Direct Test of Field Quantization in a Cavity, Phys. Rev. Lett. **76,** 1800 (1996).

[7] T. Peyronel, O. Firstenberg, Q.-Y. Liang, S. Hofferberth, A. V. Gorshkov, T. Pohl, M. D. Lukin, and V. Vuletić, Quantum nonlinear optics with single photons enabled by strongly interacting atoms, Nature (London) **488,** 57 (2012).

[8] A. Wallraff, D. I. Schuster, A. Blais, L. Frunzio, R.-S. Huang, J. Majer, S. Kumar, S. M. Girvin, and R. J. Schoelkopf, Strong coupling of a single photon to a superconducting qubit using circuit quantum electrodynamics, Nature (London) **431,** 162 (2004).

[9] A. A. Houck, D. I. Schuster, J. M. Gambetta, J. A. Schreier, B. R. Johnson, J. M. Chow, L. Frunzio, J. Majer, M. H. Devoret, S. M. Girvin, and R. J. Schoelkopf, Generating single microwave photons in a circuit, Nature (London) **449,** 328 (2007).

[10] C. Lang, D. Bozyigit, C. Eichler, L. Steffen, J. M. Fink, A. A. Abdumalikov, M. Baur, S. Filipp, M. P. da Silva, A. Blais, and A. Wallraff, Observation of Resonant Photon Blockade at Microwave Frequencies Using Correlation Function Measurements, Phys. Rev. Lett. **106,** 243601 (2011).

[11] J. Koch, T. M. Yu, J. Gambetta, A. A. Houck, D. I. Schuster, J. Majer, A. Blais, M. H. Devoret, S. M. Girvin, and R. J. Schoelkopf, Charge-insensitive qubit design derived from the Cooper pair box, Phys. Rev. A **76,** 042319 (2007).

[12] F. Motzoi, J. M. Gambetta, P. Rebentrost, and F. K. Wilhelm, Simple Pulses for Elimination of Leakage in Weakly Nonlinear Qubits, Phys. Rev. Lett. **103,** 110501 (2009).

[13] R. W. Heeres, P. Reinhold, N. Ofek, L. Frunzio, L. Jiang, M. H. Devoret, and R. J. Schoelkopf, Implementing a universal gate set on a logical qubit encoded in an oscillator, Nat. Commun. **8,** 94 (2017).

[14] P. Bertet, C. J. P. M. Harmans, and J. E. Mooij, Parametric coupling for superconducting qubits, Phys. Rev. B **73,** 064512 (2006).

[15] M. Pierre, I.-M. Svensson, S. R. Sathyamoorthy, G. Johansson, and P. Delsing, Storage and on-demand release of microwaves using superconducting resonators with tunable coupling, Appl. Phys. Lett. **104,** 232604 (2014).

[16] Y. Chen *et al.*, Qubit Architecture with High Coherence and Fast Tunable Coupling, Phys. Rev. Lett. **113,** 220502 (2014).

[17] A. Baust, E. Hoffmann, M. Haeberlein, M. J. Schwarz, P. Eder, J. Goetz, F. Wulschner, E. Xie, L. Zhong, F. Quijandría, B. Peropadre, D. Zueco, J.-J. García Ripoll, E. Solano, K. Fedorov, E. P. Menzel, F. Deppe, A. Marx, and R. Gross, Tunable and switchable coupling between two superconducting resonators, Phys. Rev. B **91,** 014515 (2015).

[18] D. C. McKay, S. Filipp, A. Mezzacapo, E. Magesan, J. M. Chow, and J. M. Gambetta, Universal Gate for Fixed-Frequency Qubits via a Tunable Bus, Phys. Rev. Applied **6,** 064007 (2016).

[19] Y. Lu, S. Chakram, N. Leung, N. Earnest, R. K. Naik, Z. Huang, P. Groszkowski, E. Kapit, J. Koch, and D. I. Schuster, Universal Stabilization of a Parametrically Coupled Qubit, Phys. Rev. Lett. **119,** 150502 (2017).

[20] M. Kounalakis, C. Dickel, A. Bruno, N. K. Langford, and G. A. Steele, Tuneable hopping and nonlinear cross-Kerr

interactions in a high-coherence superconducting circuit, npj Quantum Inf. **4,** 38 (2018).

[21] C. Eichler and J. R. Petta, Realizing a Circuit Analog of an Optomechanical System with Longitudinally Coupled Superconducting Resonators, Phys. Rev. Lett. **120,** 227702 (2018).

[22] M. J. Hartmann, Quantum simulation with interacting photons, J. Opt. **18,** 104005 (2016).

[23] C. Noh and D. G. Angelakis, Quantum simulations and many-body physics with light, Rep. Prog. Phys. **80,** 016401 (2017).

[24] M. J. Hartmann, F. G. S. L. Brandão, and M. B. Plenio, Strongly interacting polaritons in coupled arrays of cavities, Nat. Phys. **2,** 849 (2006).

[25] C. Noh, S. R. Clark, D. Jaksch, and D. G. Angelakis, Out-of-Equilibrium Physics in Driven Dissipative Photonic Resonator Arrays, in *Quantum Simulations with Photons and Polaritons*, Quantum Science and Technology (Springer, Cham, 2017), pp. 43–70.

[26] M. Abbarchi, A. Amo, V. G. Sala, D. D. Solnyshkov, H. Flayac, L. Ferrier, I. Sagnes, E. Galopin, and A. Lemaître, G. Malpuech, and J. Bloch, Macroscopic quantum self-trapping and Josephson oscillations of exciton polaritons, Nat. Phys. **9,** 275 (2013).

[27] C. Eichler, Y. Salathé, J. Mlynek, S. Schmidt, and A. Wallraff, Quantum-Limited Amplification and Entanglement in Coupled Nonlinear Resonators, Phys. Rev. Lett. **113,** 110502 (2014).

[28] C. Vaneph, A. Morvan, G. Aiello, M. Féchant, M. Aprili, J. Gabelli, and J. Estève, Observation of the Unconventional Photon Blockade in the Microwave Domain, Phys. Rev. Lett. **121,** 043602 (2018).

[29] H. J. Snijders, J. A. Frey, J. Norman, H. Flayac, V. Savona, A. C. Gossard, J. E. Bowers, M. P. van Exter, D. Bouwmeester, and W. Löffler, Observation of the Unconventional Photon Blockade, Phys. Rev. Lett. **121,** 043601 (2018).

[30] M. Fitzpatrick, N. M. Sundaresan, A. C. Y. Li, J. Koch, and A. A. Houck, Observation of a Dissipative Phase Transition in a One-Dimensional Circuit QED Lattice, Phys. Rev. X **7,** 011016 (2017).

[31] J. Raftery, D. Sadri, S. Schmidt, H. E. Türeci, and A. A. Houck, Observation of a Dissipation-Induced Classical to Quantum Transition, Phys. Rev. X **4,** 031043 (2014).

[32] P. Roushan *et al.*, Chiral ground-state currents of interacting photons in a synthetic magnetic field, Nat. Phys. **13,** 146 (2017).

[33] P. Roushan *et al.*, Spectroscopic signatures of localization with interacting photons in superconducting qubits, Science **358,** 1175 (2017).

[34] R. Ma, B. Saxberg, C. Owens, N. Leung, Y. Lu, J. Simon, and D. I. Schuster, A dissipatively stabilized Mott insulator of photons, Nature (London) **566,** 51 (2019).

[35] D. E. Chang, V. Gritsev, G. Morigi, V. Vuletić, M. D. Lukin, and E. A. Demler, Crystallization of strongly interacting photons in a nonlinear optical fibre, Nat. Phys. **4,** 884 (2008).

[36] M. J. Hartmann, Polariton Crystallization in Driven Arrays of Lossy Nonlinear Resonators, Phys. Rev. Lett. **104,** 113601 (2010).

[37] J. Jin, D. Rossini, R. Fazio, M. Leib, and M. J. Hartmann, Photon Solid Phases in Driven Arrays of Nonlinearly Coupled Cavities, Phys. Rev. Lett. **110,** 163605 (2013).

[38] J. Jin, D. Rossini, M. Leib, M. J. Hartmann, and R. Fazio, Steady-state phase diagram of a driven QED-cavity array with cross-Kerr nonlinearities, Phys. Rev. A **90,** 023827 (2014).

[39] See Supplemental Material at http://link.aps.org/supplemental/10.1103/PhysRevLett.122.183601 for information about the parametric modulation, the detection process, and the measurement of the Kerr rates, which includes Refs. [40–42].

[40] A. Kamal, A. Marblestone, and M. Devoret, Signal-to-pump back action and self-oscillation in double-pump Josephson parametric amplifier, Phys. Rev. B **79,** 184301 (2009).

[41] C. Lang, C. Eichler, L. Steffen, J. M. Fink, M. J. Woolley, A. Blais, and A. Wallraff, Correlations, indistinguishability and entanglement in Hong–Ou–Mandel experiments at microwave frequencies, Nat. Phys. **9,** 345 (2013).

[42] C. Eichler, D. Bozyigit, and A. Wallraff, Characterizing quantum microwave radiation and its entanglement with superconducting qubits using linear detectors, Phys. Rev. A **86,** 032106 (2012).

[43] L. Tian, M. S. Allman, and R. W. Simmonds, Parametric coupling between macroscopic quantum resonators, New J. Phys. **10,** 115001 (2008).

[44] D. Bozyigit, C. Lang, L. Steffen, J. M. Fink, C. Eichler, M. Baur, R. Bianchetti, P. J. Leek, S. Filipp, M. P. da Silva, A. Blais, and A. Wallraff, Antibunching of microwave-frequency photons observed in correlation measurements using linear detectors, Nat. Phys. **7,** 154 (2011).

[45] C. Eichler, J. Mlynek, J. Butscher, P. Kurpiers, K. Hammerer, T. J. Osborne, and A. Wallraff, Exploring Interacting Quantum Many-Body Systems by Experimentally Creating Continuous Matrix Product States in Superconducting Circuits, Phys. Rev. X **5,** 041044 (2015).

[46] J. Johansson, P. Nation, and F. Nori, QuTiP: An open-source Python framework for the dynamics of open quantum systems, Comput. Phys. Commun. **183,** 1760 (2012).

[47] P. Fendley, K. Sengupta, and S. Sachdev, Competing density-wave orders in a one-dimensional hard-boson model, Phys. Rev. B **69,** 075106 (2004).

[48] O. T. Brown and M. J. Hartmann, Localization to delocalization crossover in a driven nonlinear cavity array, New J. Phys. **20,** 055004 (2018).

[49] T. Fink, A. Schade, S. Höfling, C. Schneider, and A. İmamoğlu, Signatures of a dissipative phase transition in photon correlation measurements, Nat. Phys. **14,** 365 (2018).

[50] I. Carusotto and C. Ciuti, Quantum fluids of light, Rev. Mod. Phys. **85,** 299 (2013).

[51] I. M. Georgescu, S. Ashhab, and F. Nori, Quantum simulation, Rev. Mod. Phys. **86,** 153 (2014).

[52] S. Schmidt and J. Koch, Circuit QED lattices: Towards quantum simulation with superconducting circuits, Ann. Phys. (Amsterdam) **525,** 395 (2013).

[53] A. A. Houck, H. E. Türeci, and J. Koch, On-chip quantum simulation with superconducting circuits, Nat. Phys. **8,** 292 (2012).

[54] C. Gross and I. Bloch, Quantum simulations with ultracold atoms in optical lattices, Science **357,** 995 (2017).

[55] T. Prosen and I. Pižorn, Quantum Phase Transition in a Far-from-Equilibrium Steady State of an *XY* Spin Chain, Phys. Rev. Lett. **101,** 105701 (2008).

[56] M. Leib and M. J. Hartmann, Synchronized Switching in a Josephson Junction Crystal, Phys. Rev. Lett. **112,** 223603 (2014).

[57] A. Le Boité, G. Orso, and C. Ciuti, Steady-State Phases and Tunneling-Induced Instabilities in the Driven Dissipative Bose-Hubbard Model, Phys. Rev. Lett. **110,** 233601 (2013).

[58] E. M. Kessler, G. Giedke, A. İmamoğlu, S. F. Yelin, M. D. Lukin, and J. I. Cirac, Dissipative phase transition in a central spin system, Phys. Rev. A **86,** 012116 (2012).

[59] A. Biella, F. Storme, J. Lebreuilly, D. Rossini, R. Fazio, I. Carusotto, and C. Ciuti, Phase diagram of incoherently driven strongly correlated photonic lattices, Phys. Rev. A **96,** 023839 (2017).

[60] D. L. Underwood, W. E. Shanks, J. Koch, and A. A. Houck, Low-disorder microwave cavity lattices for quantum simulation with photons, Phys. Rev. A **86,** 023837 (2012).

[61] M. Elliott, J. Joo, and E. Ginossar, Designing Kerr interactions using multiple superconducting qubit types in a single circuit, New J. Phys. **20,** 023037 (2018).

[62] H. Busche, P. Huillery, S. W. Ball, T. Ilieva, M. P. A. Jones, and C. S. Adams, Contactless nonlinear optics mediated by long-range Rydberg interactions, Nat. Phys. **13,** 655 (2017).

[63] J. Tangpanitanon, S. R. Clark, V. M. Bastidas, R. Fazio, D. Jaksch, and D. G. Angelakis, Hidden order in quantum many-body dynamics of driven-dissipative nonlinear photonic lattices, Phys. Rev. A **99,** 043808 (2019).

[64] B. Peropadre, D. Zueco, F. Wulschner, F. Deppe, A. Marx, R. Gross, and J. J. García-Ripoll, Tunable coupling engineering between superconducting resonators: From sidebands to effective gauge fields, Phys. Rev. B **87,** 134504 (2013).

[65] J. Léonard, A. Morales, P. Zupancic, T. Esslinger, and T. Donner, Supersolid formation in a quantum gas breaking a continuous translational symmetry, Nature (London) **543,** 87 (2017).

[66] Y.-X. Huang, X.-F. Zhou, G.-C. Guo, and Y.-S. Zhang, Extended Bose-Hubbard model with pair hopping induced by a quadratically coupled optomechanical system, Phys. Rev. A **94,** 043842 (2016).